Cation [M = H^+, Li^+, Na^+, K^+, Ca^{2+}, Mg^{2+}, NH_4^+, and NMe_4^+] Interactions with the Aromatic Motifs of Naturally Occurring Amino Acids: A Theoretical Study†

A. Srinivas Reddy and G. Narahari Sastry*

Molecular Modeling Group, Organic Chemical Sciences, Indian Institute of Chemical Technology, Tarnaka, Hyderabad 500 007, India

Received: May 13, 2005; In Final Form: August 3, 2005

Ab initio (HF, MP2, and CCSD(T)) and DFT (B3LYP) calculations were done in modeling the cation (H^+, Li^+, Na^+, K^+, Ca^{2+}, Mg^{2+}, NH_4^+, and NMe_4^+) interaction with aromatic side chain motifs of four amino acids (viz., phenylalanine, tyrosine, tryptophan and histidine). As the metal ion approaches the π-framework of the model systems, they form strongly bound cation-π complexes, where the metal ion is symmetrically disposed with respect to all ring atoms. In contrast, proton prefers to bind covalently to one of the ring carbons. The NH_4^+ and NMe_4^+ ions have shown N−H···π interaction and C−H···π interaction with the aromatic motifs. The interaction energies of N−H···π and C−H···π complexes are higher than hydrogen bonding interactions; thus, the orientation of aromatic side chains in protein is effected in the presence of ammonium ions. However, the regioselectivity of metal ion complexation is controlled by the affinity of the site of attack. In the imidazole unit of histidine the ring nitrogen has much higher metal ion (as well as proton) affinity as compared to the π-face, facilitating the in-plane complexation of the metal ions. The interaction energies increase in the order of **1-M** < **2-M** < **3-M** < **4-M** < **5-M** for all the metal ion considered. Similarly, the complexation energies with the model systems decrease in the following order: Mg^{2+} > Ca^{2+} > Li^+ > Na^+ > K^+ ≅ NH_4^+ > NMe_4^+. The variation of the bond lengths and the extent of charge transfer upon complexation correlate well with the computed interaction energies.

Introduction

Intermolecular interactions involving aromatic rings are playing important role in both chemical and biological recognition.[1] In particular, the significance and importance of cation−π interactions between aromatic rings and metal ions was widely recognized and studied in recent years. In biological systems, a large number of metal and cationic motifs interact with proteins, nucleic acids, and enzymes.[2] Although the inter- and intramolecular noncovalent interactions including electrostatic, hydrogen bond, London, Pauli, and electron charge-transfer contributions are known to play important role, we still have a limited appreciation of their precise nature and of the way in which they compete or reinforce one another.[3] Metal ions play a key role in wide ranging biological processes, such as the regulation of enzyme, stabilization, and function of nucleic acids. They are essential for the folding and stability of large RNA molecules and proteins that form complex and compact structures.[4] These ions can modify electron flow in a substrate or enzyme, thus effectively controlling an enzyme-catalyzed reaction. The interaction of a metal cation with the π system of aromatic residues is arguably the strongest noncovalent interaction and is comparable with some of the covalent bonds.[5] Electrostatic interaction and induction are two important components for the metal ion−aromatic interaction. As a starting point, it is important to obtain reliable estimates of the binding affinities of the cations and metal ions to the aromatic−π motifs of the naturally occurring amino acids.[6] While the evidence and importance of cation−π interactions in biomolecules continues to increase in recent times, the crucial role of such interactions was widely recognized in organometallic systems for a long time.[7] The binding of proton and metal ion to biologically interesting systems such as polyamines shows contrasting trends.[8] In the past decade or so, the significance of cation−π interactions in the design of organic nanotubes, ionophores, and models for biological receptors has been clearly demonstrated.[9] Realizing the significance of cation−π interactions seem to be an important breakthrough in understanding molecular recognition. Within the protein also we can find the cation−π interactions between the cationic side chains of the either lysine or arginine and the aromatic side chains of phenylalanine, tyrosine, tryptophan, and histidine.

SCHEME 1

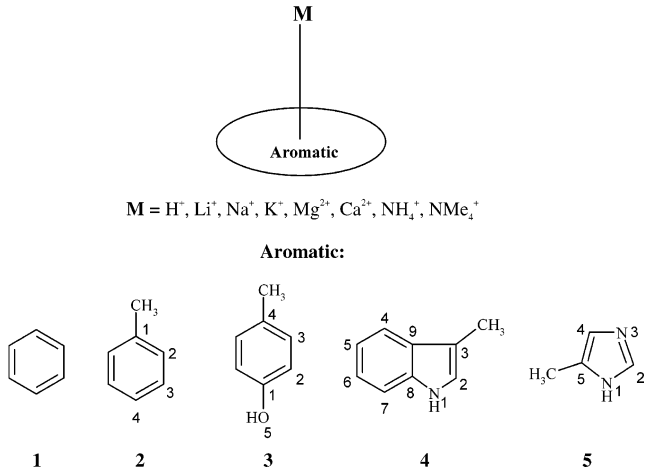

† This is IICT Communication No. 050208.

* Corresponding author e-mail: gnsastry@iict.res.in or gnsastry@yahoo.com.

10.1021/jp0525179 CCC: $30.25 © 2005 American Chemical Society
Published on Web 09/09/2005

TABLE 1: Comparison of Experimental and Various Computational Estimates of Metal Ion Complexation Energy (in kcal/mol) with Benzene

S no.	method	Li^+	Na^+	K^+
1	[j]EXP	−37.90[a]	−28.00 ± 1.50[b]	−19.20[c]
2	[d]CID-GIBMS	−38.50 ± 3.23	−22.13 ± 1.39	−17.52 ± 0.91
3	[j,e]CCSD(T)/CBS	−36.80 ± 0.20	−24.70 ± 0.30	−20.10 ± 0.40
4	[j,f]BP86/TZ94P	−33.60	−21.00	−13.00
5[k]	[d]MP2 (full)/6-311+G**//MP2 (full)/6-31G*	−34.30	−21.37	−17.09
6[k]	[j,f]MP2/6-311+G*	−35.00	−21.00	−16.00
7[k]	[g]MP2/6-31+G*	−34.60	−22.14	−15.47
8[k]	[h]B3LYP/6-31++G**	−35.35	−23.16	−14.90
9[k]	[h]MP2/6-31++G**	−31.66	−20.07	−16.17
10[k]	[i]B3LYP/6-311++G**	−36.12	−22.24	−15.20
11[k]	[i]MP2/6-311++G**	−33.76	−20.42	−16.31
12[k]	[i]B3LYP/6-31G**	−38.10	−25.39	−15.52
13[k]	[i]MP2/6-31G**	−36.94	−24.39	−16.36
14[k]	[i]CCSD(T)/6-31G**	−41.56	−28.06	−19.09

[a] Ref 12. [b] Ref 13. [c] Ref 14. [d] Ref 15; bond dissociation energies at 0 K. [e] Ref 16a. [f] Ref 16c. [g] Ref 17. [h] Ref 22a. [i] Present work. [j] Enthalpies calculated at 298 K. [k] Entries 5−14 are values corrected for BSSE.

It becomes very important to quantify the strength of interactions present in amino acid side chains that sculpt the peptides. There have been a number of experimental and theoretical studies reported in the literature aimed at determining the strength of cation−π interactions between a variety of metal cations and model systems such as benzene, fluorobenzene, anisole, nucleobases, nitrogen heterocycles, etc., which are the model prototypical systems of biomolecules.[9−17] Study of the complexion of the alkali, alkaline earth metals to the π-face of benzene has attracted many experimental and theoretical groups. Dunbar et al. using kinetic method calculated the Na^+, K^+ affinities of phenylalanine, tyrosine, and tryptophan.[18] Rodgers and co-workers[19] using the collision-induced dissociation technique has determined the bond dissociation energies of cation−π complexes of anisole and the alkali metal cation and also by theoretical studies at MP2(full)/6-311+G**. They have also reported the energetics of Na^+, K^+ complexes with aromatic amino acids such as phenylalanine, tyrosine, and tryptophan using the guided ion beam tandem mass spectrometry method.[19] Zhu et al. have employed B3LYP/6-311++G** calculations to systematically explore the geometrical multiplicity and binding strength for the alkali and alkaline earth metal complexes with nucleobases (namely, adenine, cytosine, guanine, thiamine, and uracil).[20] Sponer and co-workers also have reported the HF and MP2 computations on the interaction of mono- and divalent metal ions with nucleobases.[21] Garau and co-workers[22] have studied the nonbonded interactions of different anions with benzene using a topological analysis of the electron density and molecular interaction potential with polarization (MIP_p) energy partition scheme calculations. Further quantitative estimation of cation−π and anion−π interactions was carried out, emphasizing the changes in the aromaticity of the ring upon complexation and charge-transfer.[22] Tsuzuki et al. examined the dependence of basis set quality, electron correlation, and structural variations on the interaction of the alkaline−earth metal divalent cations with benzene.[23] Ikuta and co-workers have described the interaction between the monovalent cations (Li^+, Na^+, and K^+) with anthracene and phenanthrene molecules at the hybrid DFT.[24]

However, to our knowledge, a systematic study of binding of alkali and alkaline earth metals to the aromatic side chain motifs of proteins with a special attention to cation−π interactions has not yet been reported, barring some isolated reports.[17,19] Even though it is practical to carry out sophisticated post-SCF quantum mechanical calculations on the benzene system, it may not truly represent the aromatic behavior of all the aromatic amino acid side chains. Considering the contemporary interest and importance of these interactions, we ventured to perform a systematic and comprehensive study of the cation−π interactions[25] with the aromatic side chain motifs of the naturally occurring amino acids. Thus, the present study is directed toward quantifying the alkali and alkaline metal ions (Li^+, Na^+, K^+, Ca^{2+}, Mg^{2+}) along with H^+, NH_4^+, and NMe_4^+ interactions with the aromatic side chains (Scheme 1) of naturally occurring amino acids. Importantly, the present study is directed to investigate the regioselectivity of the site of attack on these aromatic side chain motifs by metal ions and protons. Computations were carried out on all the possible sites of attack. While the main aim of the paper is to present a systematic analysis of metal ion binding with the aromatic side chains and contrasting them with the proton affinity values, we also incorporate the Morokuma decomposition analysis (see Supporting Information) to discern the individual components of the interaction energy.

TABLE 2: Proton Affinities (PA) of the Aromatics Calculated at B3LYP/6-31G and CCSD(T)/6-31G** Level and the Zero Point Vibration Energy Differences (ΔZPE) between the Protonated and Neutral Complexes[a]**

	B3LYP/6-31G**			CCSD(T)/6-31G**
structure	NIMAG	PA	ΔZPE	PA
1a-H	2	−134.52	1.94	−132.48
1b-H	0	−193.81	6.28	−191.76
2a-H	0	−193.02	7.13	−192.01
2b-H	0	−201.03	6.46	−198.37
2c-H	0	−197.30	6.39	−195.02
2d-H	0	−202.24	6.37	−199.62
3a-H	0	−187.64	6.17	−186.73
3b-H	0	−210.86	7.31	−209.10
3c-H	0	−200.14	6.18	−197.03
3d-H	0	−209.16	8.02	−209.47
3e-H	0	−192.45	7.24	−197.03
4a-H	0	−216.07	8.58	−220.24
4b-H	0	−227.42	7.40	−231.29
4c-H	0	−225.22	8.29	−229.46
4d-H	0	−220.30	7.19	−220.11
4e-H	0	−220.59	7.29	−222.15
4f-H	0	−220.60	7.14	−220.64
4g-H	0	−217.69	7.37	−219.08
5a-H	0	−191.54	7.47	−195.92
5b-H	0	−215.16	7.44	−217.33
5c-H	0	−243.51	8.79	−244.77
5d-H	0	−214.56	7.00	−216.63
5e-H	0	−209.54	7.84	−212.96

[a] All the values are in kcal/mol.

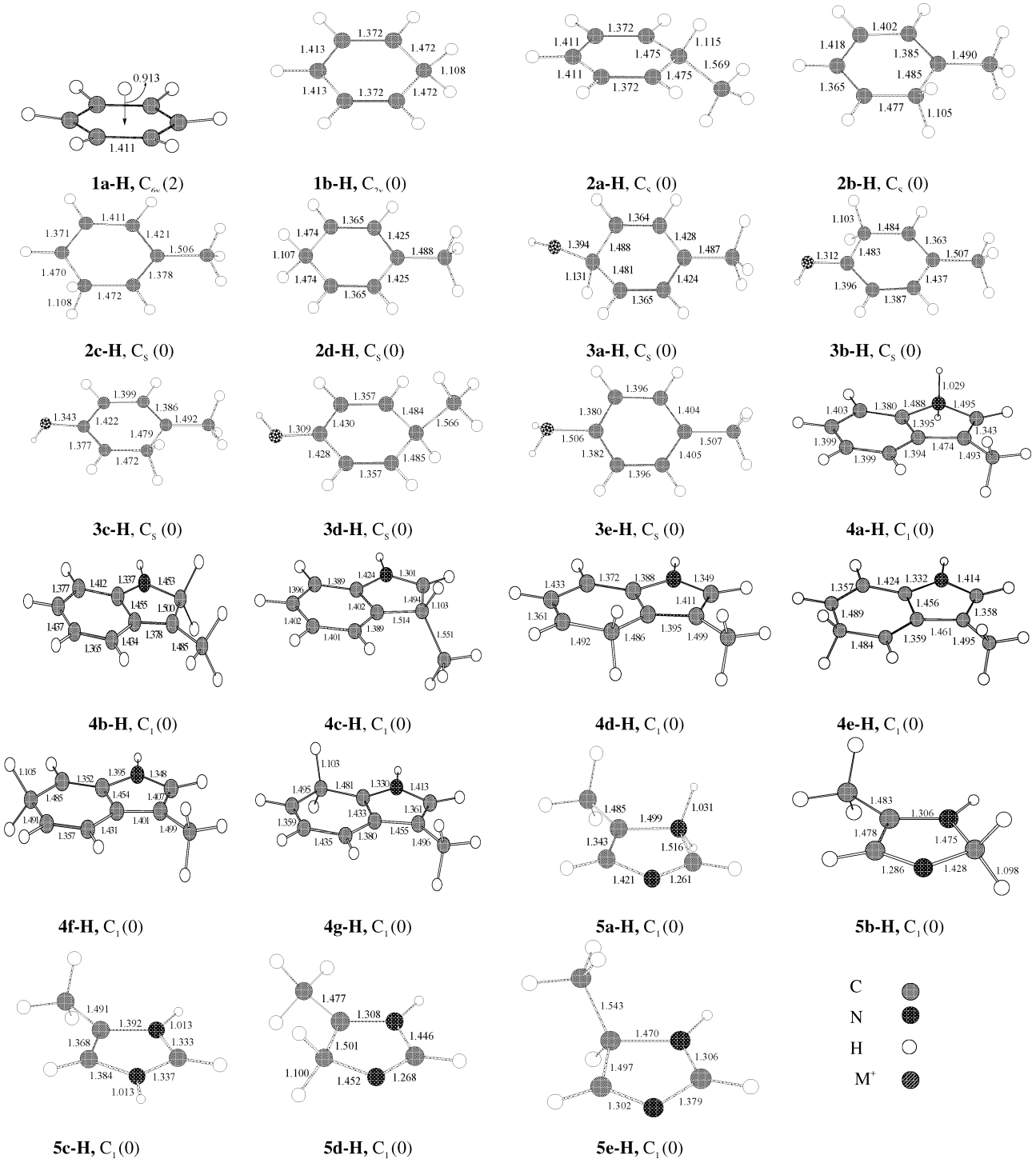

Figure 1. Optimized geometries (in Å) of all the protonated complexes at B3LYP/6-31G** level. The number of imaginary frequencies are given in parentheses.

Methods

All the structures considered in the study were initially optimized at B3LYP/6-31G** level, and the nature of the resultant stationary points is ascertained with frequency calculations. This is followed by single-point energy calculations at B3LYP and MP2 levels using the 6-311++G** basis set. The 6-31G** basis set is a split-valance double-ζ quality with one set of polarization function both on heavy atom and hydrogen, whereas 6-311++G** is a split-valance triple-ζ basis set augmented with a set of polarization and diffuse functions for both heavy atoms and hydrogens. The Boys−Bernardi counterpoise method was applied to estimate the basis set superposition error (BSSE) at various levels of theory.[26] Unscaled thermochemical data obtained at B3LYP/6-31G** level were used. The regioisomers of the protonated complexes were located to assess the relative propensity of the various sites for proton attach at B3LYP/6-31G** and at CCSD(T)/6-31G** levels of theory. All calculations were done using the Gaussian 03 suite of programs.[27] All the optimizations, except benzene complexes, are done without imposing any symmetry constrains. The complexes formed when proton or metal ion binds with the heteroatom were also located in addition to the π-complexes,

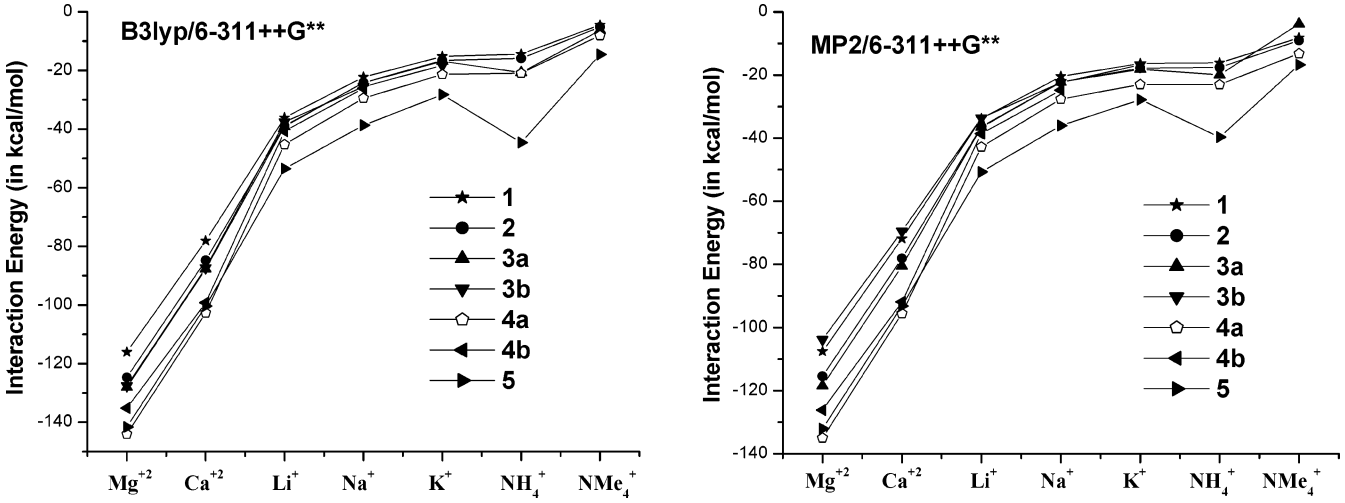

Figure 2. Interaction energy profiles of the various cation−aromatic complexes at B3LYP/6-311++G** and MP2/6-311++G** levels of theory.

where possible. The proton affinity and metal ion affinities were calculated as given below:

$$\text{aromatics} + M^+ \rightleftarrows \text{complex}$$

$$\text{proton affinity } (\Delta H_{298}) = \Delta E_{ele} + \Delta ZPE$$

$$\text{metal ion affinity } (\Delta H_{298}) = \Delta E_{ele} + \Delta ZPE + BSSE$$

where $\Delta E_{ele} = E_{complex} - (E_{aromatic} + E_{M^+})$. The contribution of electron correlation for a given basis set is estimated as the difference between the interaction energies calculated at MP2 and HF levels of theory. Similarly, the difference between the MP2 and B3LYP interaction energies is considered as the dispersion energy as has been reported earlier.[22a] The contribution of electron correlation and dispersion terms to the interaction energy was evaluated using 6-311++G** basis sets.

Results and Discussion

The results of the present work are organized in the following way. First, the applicability of theoretical methods to the larger systems is assessed based on the studies of the model system benzene. This is followed by a description of protonation energies and the site selectivity of the proton on the aromatic motifs. Then, the relative complexation energies of cation−π and cation−heteroatom interactions are compared and analyzed. Structural variations upon metal ion complexation are also analyzed. The complexation energy variations as a function of metal ion and the aromatic motif is analyzed next.

The earlier experimental and computed metal ion (Li^+, Na^+, and K^+) affinities to the benzene ring are summarized in Table 1. In the present work, interaction energies are calculated for alkali metal cations (Li^+, Na^+, and K^+) with benzene at HF, B3LYP, and MP2 levels of theory using 6-31G** and 6-311++G** basis sets and at the CCSD(T)/6-31G** level. The interaction energies corrected for BSSE and ZPE calculated at B3LYP/6-311++G** and MP2/6-311++G** levels of theory are in good agreement with the experimental results reported by the Armentrout group[15] and are also consistent with the earlier theoretical studies. Encouragingly, the trends obtained at various levels of theory are essentially similar, albeit with small quantitative differences.

Regioselectivity of Proton. To locate the preferable site for protonation on these motifs, we have computed the proton affinities at all the possible sites of the π-framework. The calculated proton affinities at both B3LYP/6-31G** and CCSD(T)/6-31G** levels of theory are summarized in Table 2. The optimized geometries of these complexes at B3LYP/6-31G** level of theory are given in Figure 1. The symmetrical **1a-H** complex, in which proton is along the principal axis of symmetry of benzene is at a distance of 0.91 Å from the centroid of the aromatic ring, is characterized as a second-order saddle point on the potential energy surface, as has been reported earlier. In contrast, **1b-H** is a minima, where the proton is covalently bound to one of the ring carbon atoms, and this covalently bound complex is computed to be much more stable compared to the π-complex **1a-H**.

In toluene, the sites C2 and C3 have the same proton affinity, and the corresponding protonated complexes **2b-H** and **2d-H** are more stable among the four (**2a-H**, **2b-H**, **2c-H,** and **2d-H**) possible protonated complexes, as the carbocation formed is stabilized by presence of methyl group. Similarly, *p*-hydroxy toluene has five plausible sites for protonation, and the respective protonated complexes are **3a-H**, **3b-H**, **3c-H**, **3d-H**, and **3e-H**. Among them the sites C2 (**3b-H**) and C4 (**3d-H**) possess high proton affinity, which may be traced to the hyperconjugative stabilization of the formed carbocation by the hydroxyl and methyl groups. Among seven possible protonated methyl indole complexes, **4b-H** is the most stable, where the protonation has taken place at the C2 site present in the five-membered ring followed by **4c-H**. The proton affinities of the C4, C5, C6, and C7 sites of the six-membered ring and C1 site of the five-membered ring are very similar. The **4b-H** complex is obviously stable as the secondary carbocation formed get stabilized due to the electron donation from the adjacent N lone pair, while **4c-H** is also equally competitive, due to the formation of stable tertiary carbocation. However, such extra stabilizations are not possible when the proton complexes with the other sites. Therefore the remaining sites (C1, C4, C5, C6, and C7) have about 10−12 kcal/mol lower proton affinities as compared to the sites with the highest proton affinity. In case of methyl imidazole, evidently, the lone pair bearing basic nitrogen center N3 (**5c-H**) has the highest proton affinity (−244.77 kcal/mol) among all the available sites. Proton affinity values of the other centers except C1 are approximately 30 kcal/mol lower as compared to the nitrogen center. The C1 site proton affinity is about 50 kcal/mol lower as compared to the N3 site affinity. These values are much higher compared to the complexation on benzene.

TABLE 3: Interaction Energies, BSSE Values for 2-M, 3-M, 4-M, and 5-M Complexes at B3LYP/6-31G, B3LYP/6-311++G**, and MP2/6-311++G** Levels of Theory along with the Zero Point Vibration Energy Differences (ΔZPE) between the Complexed and Neutral Aromatics, Correlation Energies (E_{cor}), and Dispersion Energies (E_{dis})[a]**

	B3LYP					MP2			
	6-31G**			6-311++G**		6-311++G**			
structure	IE	ΔZPE	BSSE	IE	BSSE	IE	BSSE	E_{cor}	E_{dis}
1-Li	−38.10	1.65	2.50	−36.12	0.55	−33.76	4.35	−1.70	−1.44
1-Na	−25.39	0.90	2.12	−22.24	0.71	−20.42	3.73	−2.30	−1.20
1-K	−15.52	0.68	2.21	−15.20	0.34	−16.31	2.61	−4.44	−3.38
1-Ca	−69.87	1.01	2.23	−78.08	0.28	−71.82	3.93	−5.23	2.61
1-Mg	−121.44	1.20	2.73	−116.03	0.85	−107.56	5.40	−0.77	3.92
1-NH_4	−15.71	0.90	0.88	−14.49	0.39	−16.05	2.29	−5.97	−3.46
1-NMe_4	−5.54	0.65	1.29	−4.52	0.48	−8.16	2.97	−7.00	−6.13
2-Li	−40.71	1.84	2.33	−38.90	0.57	−36.36	4.27	−1.61	−1.16
2-Na	−27.06	1.03	2.05	−24.18	0.69	−22.18	3.65	−2.24	−0.96
2-K	−16.64	0.78	2.11	−16.59	0.34	−17.80	2.68	−4.73	−3.55
2-Ca	−75.34	1.06	2.17	−84.78	0.41	−78.11	3.94	−5.80	3.14
2-Mg	−129.63	1.24	2.61	−124.69	0.88	−115.45	5.33	−1.08	4.79
2-NH_4	−16.94	1.05	0.96	−15.90	0.41	−17.57	2.30	−6.46	−3.56
2-NMe_4	−6.09	0.75	1.30	−5.19	0.45	−9.01	3.01	−7.43	−6.38
3a-Li	−41.28	1.77	2.39	−39.11	0.62	−36.51	4.22	−2.02	−1.00
3a-Na	−27.34	0.97	2.24	−24.17	0.81	−22.19	3.72	−2.69	−0.93
3a-K	−17.06	0.67	2.19	−16.86	0.37	−18.14	2.71	−5.14	−3.62
3a-Ca	−77.96	1.00	2.29	−87.71	0.45	−80.51	3.99	−7.12	3.66
3a-Mg	−134.32	1.25	2.68	−127.99	0.94	−118.42	5.26	−2.78	5.25
3a-NH_4	−22.01	0.75	1.37	−20.70	0.71	−19.93	2.75	−5.29	−1.27
3a-NMe_4	−6.81	0.71	2.39	−6.32	1.64	−3.76	9.52	−7.24	−6.03
3b-Li	−39.63	0.99	2.94	−37.59	0.60	−34.97	2.83	−1.17	0.39
3b-Na	−27.63	0.50	2.66	−25.55	0.71	−23.58	2.59	−1.16	0.09
3b-K	−18.06	0.38	2.31	−18.28	0.26	−18.80	2.01	−3.24	−2.27
3b-Ca	−79.68	0.34	2.58	−87.36	0.21	−80.90	2.97	−6.30	4.51
3b-Mg	−132.56	0.23	3.15	−127.59	0.85	−115.77	3.56	−2.77	9.11
4a-Li	−47.58	1.85	2.28	−45.25	0.64	−42.76	4.51	−2.89	−1.38
4a-Na	−32.66	0.99	2.09	−29.46	0.84	−27.61	4.00	−3.41	−1.31
4a-K	−21.41	0.72	2.04	−21.37	0.36	−22.95	2.97	−6.00	−4.19
4a-Ca	−91.03	1.05	2.17	−102.66	0.45	−95.56	4.38	−9.59	3.17
4a-Mg	−149.99	1.19	2.57	−144.04	0.99	−134.98	5.73	−5.12	4.32
4a-NH_4	−22.22	0.94	0.94	−20.92	0.48	−23.01	2.64	−8.14	−4.25
4a-NMe_4	−9.05	0.72	1.37	−8.10	0.66	−13.16	4.00	−9.80	−8.40
4b-Li	−43.03	1.68	2.11	−40.70	0.61	−38.54	3.91	−2.28	−1.14
4b-Na	−28.87	0.81	1.94	−26.13	0.85	−24.77	3.63	−2.53	−1.42
4b-Ca	−85.79	0.92	1.98	−99.18	0.29	−91.86	4.24	−7.83	3.37
4b-Mg	−140.48	0.72	2.40	−135.12	0.98	−126.15	4.93	−3.59	5.02
5-Li	−53.91	1.69	2.93	−53.55	0.37	−50.69	1.79	0.80	1.44
5-Na	−39.92	1.06	2.61	−38.72	0.48	−36.02	1.70	−0.05	1.48
5-K	−27.91	0.80	2.41	−28.28	0.18	−27.75	1.48	−2.12	−0.77
5-Ca	−92.17	1.14	2.70	−100.34	0.23	−93.16	1.99	−2.86	5.42
5-Mg	−144.39	1.35	3.19	−141.60	0.71	−132.05	2.29	0.26	7.97
5-NH_4	−46.73	0.82	1.54	−44.57	0.49	−39.66	3.41	−2.36	1.99
5-NMe_4	−15.20	1.05	2.11	−14.51	0.29	−16.68	2.06	−5.48	−3.94

[a] All values are given in kcal/mol. E_{cor} and E_{dis} are calculated using 6-311++G** basis set.

The trends obtained of all the possible sites appear to be independent of method (B3LYP, HF, MP2, or CCSD(T)) or the basis set. While quantitative discrepancies do exist, they are not very significant. The ZPE values of all the protonated complexes calculated at B3LYP/6-31G** level are in the range of 6−9 kcal/mol, except for **1a-H**. The **5c-H** complex, which is the most stable among all the protonated complexes, has the higher ZPE value of 8.79 kcal/mol. The complex **1a-H** has the lowest ZPE value of 1.94 kcal/mol.

Cation Complexes. The interaction energies of cations (Li^+, Na^+, K^+, Mg^{2+}, Ca^{2+}, NH_4^+, NMe_4^+) with the aromatic motifs are calculated at HF, MP2, and B3LYP levels of theory using 6-31G** and 6-311++G** basis sets. The expensive CCSD(T) calculations could not be carried out as they are prohibitively expensive. Metal ion found to bind to the aromatic motifs either through cation−π interaction or cation−heteroatom interaction. None of the cases yielded a stationary point correspond to the situation where the metal ion is bound covalently to only one of the C atoms of the ring. The cation is attracted by the high electronegative heteroatom if it is present in the aromatic system. In case of NH_4^+ and NMe_4^+, hydrogen bond complexes are formed with the heteroatoms. But in the absence of heteroatom, the $NH4^+$ and NMe_4^+ ions have shown a strong interaction with the π−electron cloud of the aromatic rings. These N−H$\cdots\pi$ and C−H$\cdots\pi$ interactions are competitive in strength with the hydrogen bond.[28] The general trend of interaction energies of these cations with various aromatics is $Mg^{2+} > Ca^{2+} > Li^+ > Na^+ > K^+ \cong NH_4^+ > NMe_4^+$. In the case of aromatics, the interaction energies increase in the order of **1-M** < **2-M** < **3-M** < **4-M** < **5-M**, for all the metal ions considered. In Figure 2 given the interaction energy profiles of various cation−aromatic complexes at B3LYP/6-311++G** and MP2/6-311++G** levels of theory. The perpendicular distance from the cation to the aromatic motif varies accordingly with the strength of interaction.

A perusal of the bond length variation upon ion complexation reveals that there is elongation of all the ring bond lengths when the metal ion binds to the π-face. The bond lengths connecting

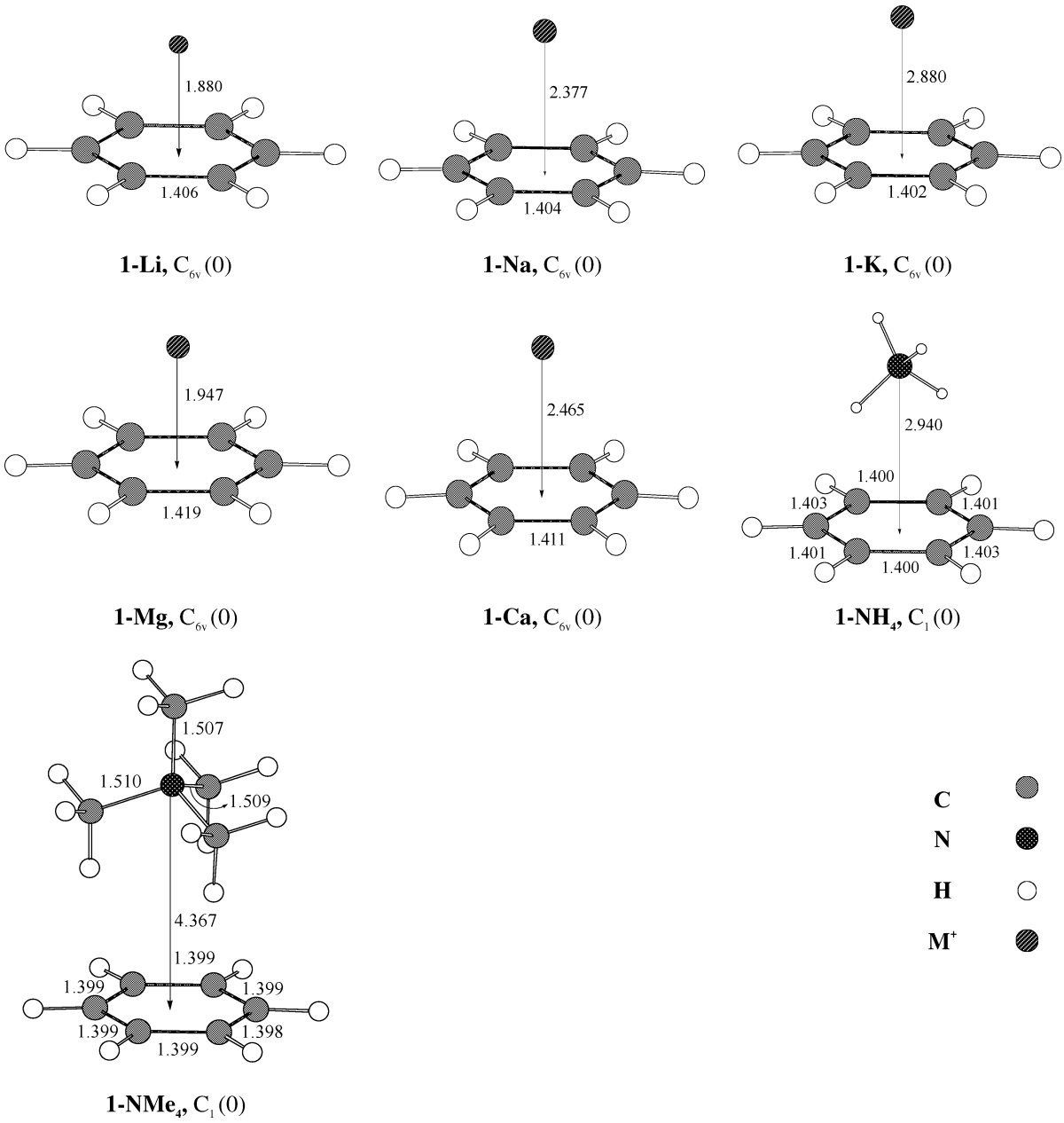

Figure 3. Optimized geometries (in Å) of **1-M** complexes at B3LYP/6-31G** level. The number of imaginary frequencies are given in parentheses.

the substituents are slightly shortened (e.g., the C−C(Me) bond length is shortened in all the complexes). It is also observed that the extent of elongation is proportional to the strength of the interaction energies. Thus, the elongation of ring bond lengths is highest for the Mg complexes and lowest for NMe_4 complexes. A maximum increase of 0.072 Å is observed in the **4a-Mg** complex. When the metal ion binds to the in plane heteroatoms, although the variations in the bond lengths are not always predictable their extent is roughly proportional to the strength of interaction.

Table 3 summarizes the interaction energies of aromatic M ($M = Li^+$, Na^+, K^+, Mg^{2+}, Ca^{2+}, NH_4^+, NMe_4^+) complexes at B3LYP/6-31G**, B3LYP/6-311++G**, and MP2/6-311++G** levels of theory along with the ΔZPE, BSSE values, the contributions of correlation energy (E_{cor}) and dispersion energy (E_{dis}) terms to the total interaction energies. Figures 3−7 contain the optimized geometries at B3LYP/6-31G** level of theory of benzene-M (**1-M**), toluene-M (**2-M**), *p*-hydroxy toluene-M (**3-M**), methyl indole-M (**4-M**), and methyl imidazole-M (**5-M**) complexes, respectively.

The effect of level of theory and basis set is there upon the interaction energy magnitudes; however, the trend remains the same at all the levels of theory. The cation affinity values of these complexes calculated using 6-31G** basis set are overestimated as compared to the interaction energies calculated using the 6-311++G** basis set, except for Ca^{2+} complexes.

1-M Complexes. Among the **1-M** complexes, the dication complexes (**1-Mg** and **1-Ca)** have more interaction energy than the other complexes. **1-Mg** complex has highest interaction energy of −107.56 kcal/mol at MP2/6-311++G** level and is 35.74 kcal/mol more than **1-Ca** complex. The dispersion energy values of these dication complexes are positive, and the distance from the cation to centroid of the aromatic ring is 1.947 and 2.465 Å, respectively. All the **1-M** complexes are minima on the potential energy surface. The relative order of the distance from the metal ion to the centroid of the aromatic ring is $Li^+ < Mg^{2+} < Na^+ < Ca^{2+} < K^+ < NH_4^+ < NMe_4^+$.

2-M Complexes. In case of toluene, the trend of interaction of cations with the π−framework is almost same as the trend of benzene. However the interaction energies of the toluene-M

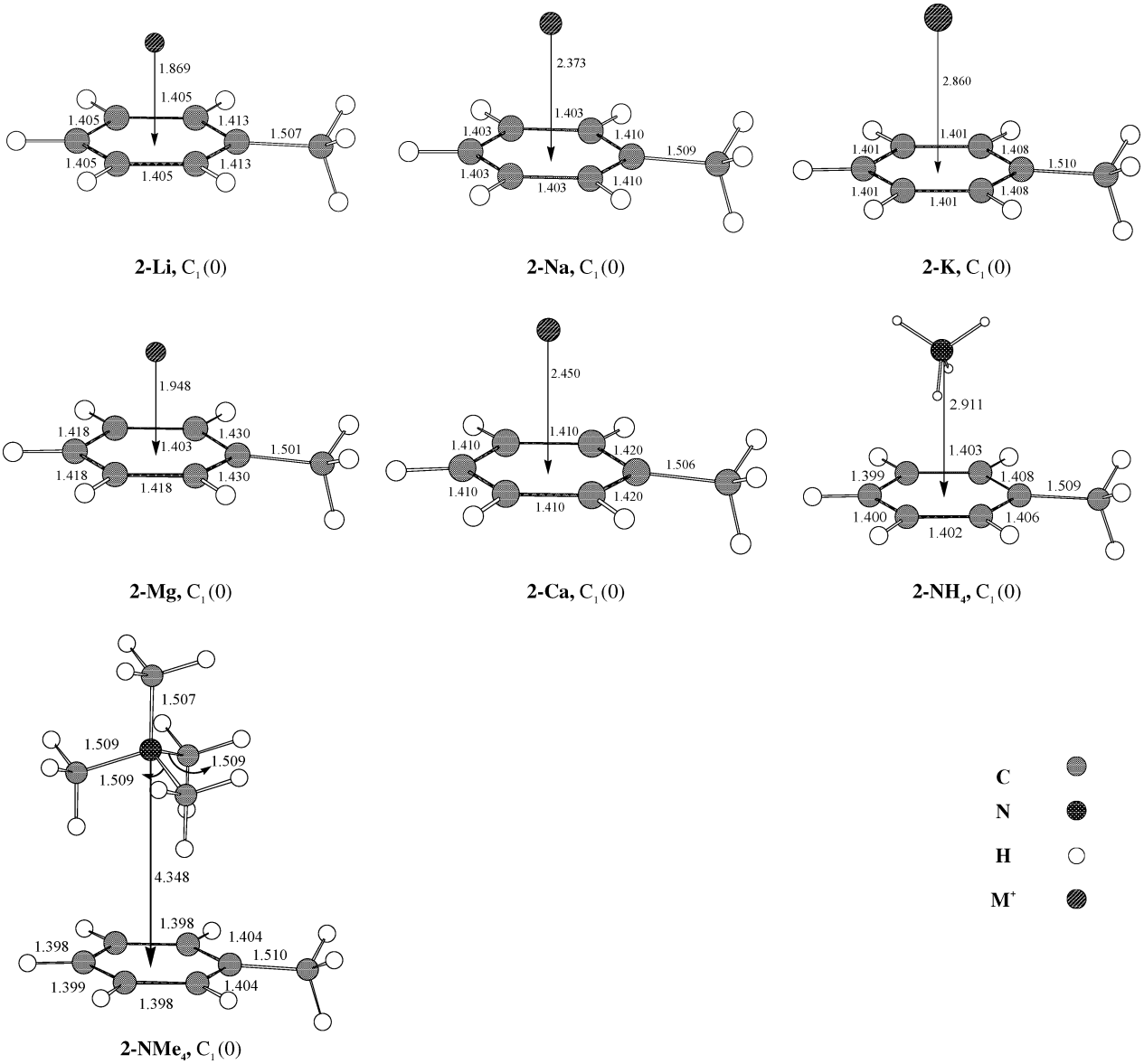

Figure 4. Optimized geometries (in Å) of **2-M** complexes at B3LYP/6-31G** level. The number of imaginary frequencies are given in parentheses.

(**2-M**) complexes are higher than the respective benzene-M (**1-M)** complexes, possibly due to the electron donating nature of the methyl group. Maximum of 7.89 kcal/mol difference is observed between the interaction energies of **2-Mg** and **1-Mg** complexes at the MP2/6-311++G** level of theory. The correlation energy values of **2-M** complexes are more than the corresponding **1-M** complexes, and again the maximum increase is observed in the **2-Mg** complex.

3-M Complexes. The side chain aromatic motif of the amino acid residue—tyrosine—is taken in this section. Effectively two competitive binding modes exist; viz. the π-interaction (**3a-M**) and the other is the cation interaction with the electronegative oxygen atom (**3b-M**). Interestingly, the π-complexation energies of the metals are very strong and similar in magnitude as compared to the σ-complexes where the metals are bound with the more electronegative oxygen atom (Table 3). In **3-M** complexes, although the trend in the interaction energies is in agreement with the general trend, due to the formation of hydrogen bond, the interaction energy of **3a-NH$_4$** complex is more than the **3a-K** complex by 2−5 kcal/mol at various levels of theory. The interaction energy trend is $Mg^{2+} > Ca^{2+} > Li^+ > Na^+ > NH_4^+ > K^+ > NMe_4^+$. The **3a-M** complexes have approximately 3−13 kcal/mol higher binding affinities than that of corresponding **2-M** complexes at B3LYP level of theory and 2−20 kcal/mol more at MP2 level of theory. The electron correlation values (E_{cor}) of **3a-M** complexes **(**M = H^+, Li^+, Na^+, K^+) are 2−3 kcal/mol higher than the corresponding **3b-M** complexes. Except for **3b-K**, all the **3b-M** complexes have positive dispersion energy values.

4-M Complexes. In methyl indole, the system contains two aromatic rings (six-membered and five-membered). There is a possibility that the cation may interact with the π−electron framework of either six-membered ring (**4a-M**) or five-membered ring (**4b-M**). All the complexes are minima on the potential energy surface. The interaction energies of **4a-M** are more than the respective interaction energies of **4b-M** by about 3−9 kcal/mol at B3LYP and MP2 level. K^+ ion could not form a complex with the five-membered aromatic π−framework. Electron correlation energy values are also higher in **4a-M** than **4b-M** complexes. Dispersion energies are positive in case of **4a-Mg**, **4b-Mg**, **4a-Ca**, and **4b-Ca** complexes. Although all the aromatics (benzene, toluene, and *p*-hydroxy toluene and methyl indole) have the six-membered aromatic rings, the interaction of cation with the six-membered ring of methyl indole is high

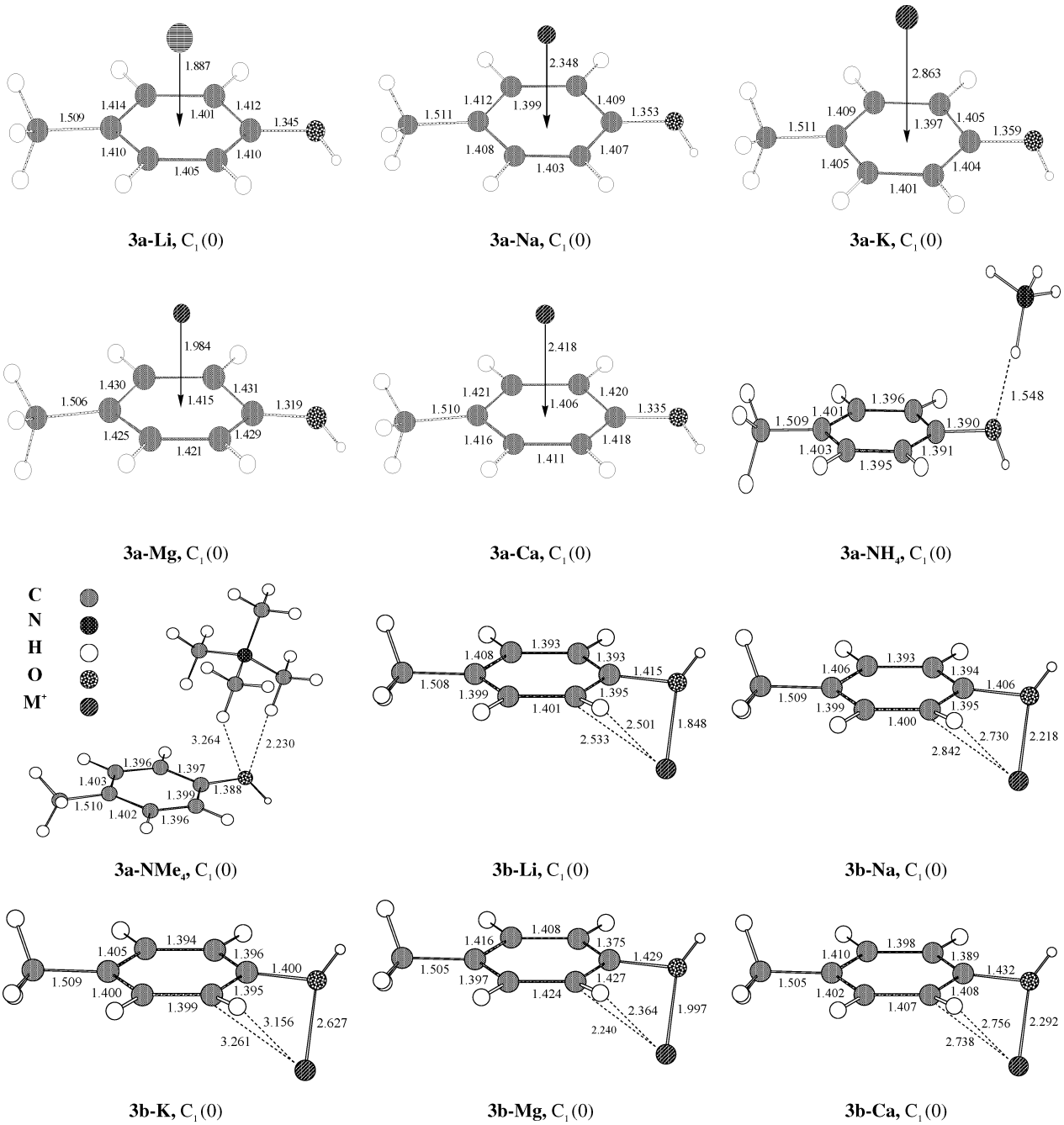

Figure 5. Optimized geometries (in Å) of **3-M** complexes at B3LYP/6-31G** level. The number of imaginary frequencies are given in parentheses.

as compared to the other because of its high aromatic nature. **4a-Mg** has around 28.5 kcal/mol more binding affinity than **1-Mg** complex at B3LYP/6-31G** and 27.42 kcal/mol at MP2/6-311++G** levels of theory.

5-M Complexes. In the case of methyl imidazole, cations have shown affinity only toward the heteroatom (lone pair bearing N3 atom) present in the ring but not to the π-face. Exhaustive efforts were made to locate the π-complex without success. All the formed complexes are characterized as minima on the potential energy surface. The interaction energies are relatively higher than the complexes of the other aromatics. The interaction energy of the **5-Mg** complex is more than the **1-Mg** complex by 24.49 kcal/mol at MP2/6-311++G** level of theory. In case of **5-NH4** and **5-NMe4** complexes, the binding energy are having approximately thrice the binding energies of **1-NH4** and **1-NMe4** complexes, respectively. This is due to the formation of hydrogen bond between the protons of NH_4^+ or NMe_4^+ with nitrogen atom of imidazole ring. So the trend of interaction energies in **5-M** complexes is slightly deviated from the regular trend. The interaction energy trend in case of methyl imidazole complexes is $Mg^{2+} > Ca^{2+} > Li^+ > NH_4^+ > Na^+ > K^+ > NMe_4^+$. The relative distance of the cation from the nitrogen atom of the ring is in the order of **5a-K** > **5a-Ca** > **5a-Na** > **5a-Mg** > **5a-Li**.

The values of the correlation correction and dispersion energies indicate that they have nonnegligible contributions. The dispersive interactions are positive for all the dications and also for monocations when they interact with the heteroatom. While the correlation energies are negative for all the π-complexes, for some of the covalently bound complexes it is positive. Therefore, electron correlation and dispersive interactions can be important components of the total interaction energies; therefore, their consideration is important to get reliable

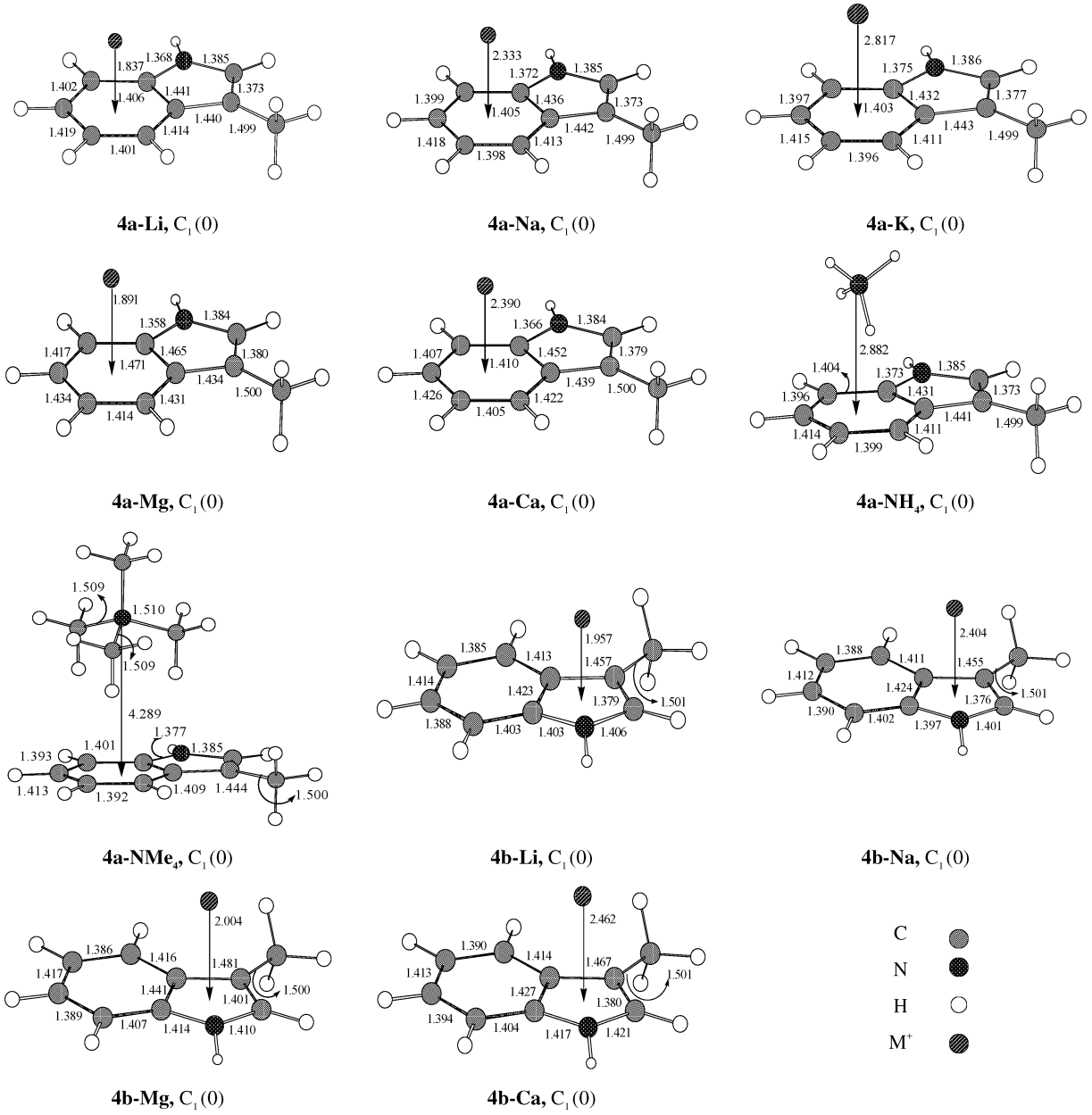

Figure 6. Optimized geometries (in Å) of **4-M** complexes at B3LYP/6-31G** level. The number of imaginary frequencies are given in parentheses.

estimates of the interactions energies. As the cation size increases, both correlation and dispersive correction values are increasing.

Charge Analysis. The Mulliken charges of the cations (Li^+, Na^+, K^+, Ca^{2+}, Mg^{2+}) in various cation−π and cation−heteroatom complexes are summarized in Table 4. From the data, we can gauge at the positive charge that has transferred from cation to the aromatic system during the interaction. It has been observed that the strength of interaction is linearly correlated with amount charge transfer, whether it is π-complex or a covalently bound complex. In case of monovalent cations, the order of charge transferred from cation to π-system is $K^+ < Na^+ < Li^+$ (i.e., from K^+ to Li^+ the charge dispersed from cation to π-system increases). This may be due to less surface area available for the cation to interact with the π-system or heteroatom. The strength of interaction decreases, as the ionic radius increases from lithium to potassium. However the amount of charge transferred from dication complexes to π-system or heteroatom is much higher as compared to the charge transferred from monocation complexes.

Among the dication complexes, Mg^{2+} has less Mulliken charge as compared to Ca^{2+} ion signifying that higher amount of charge is being transferred from cation to π-system.As a result, the highest interaction is observed in case of Mg^{2+} complexes. In case of *p*-hydroxy toluene, relatively the positive charge transferred from cation to π-system in **3a-M** complexes is more than the charge transferred to oxygen atom of the hydroxyl group in case of **3b-M** complexes. In methyl indole complexes the charge transferred from cation to six-membered aromatic ring of **4a-M** is more than the charge transferred to five-membered ring of **4b-M** following the same array of interaction energies. For that reason, we can consider the amount of charge that has been transferred from the cation to aromatic system as a scale to express the binding strength of the cation with the various aromatic motifs.

Conclusions

The present paper reports a systematic and thus far most comprehensive study on the cation (H^+, Li^+, Na^+, K^+, Mg^{2+}, Ca^{2+}, NH_4^+, and NMe_4^+) with the aromatic side chain motifs

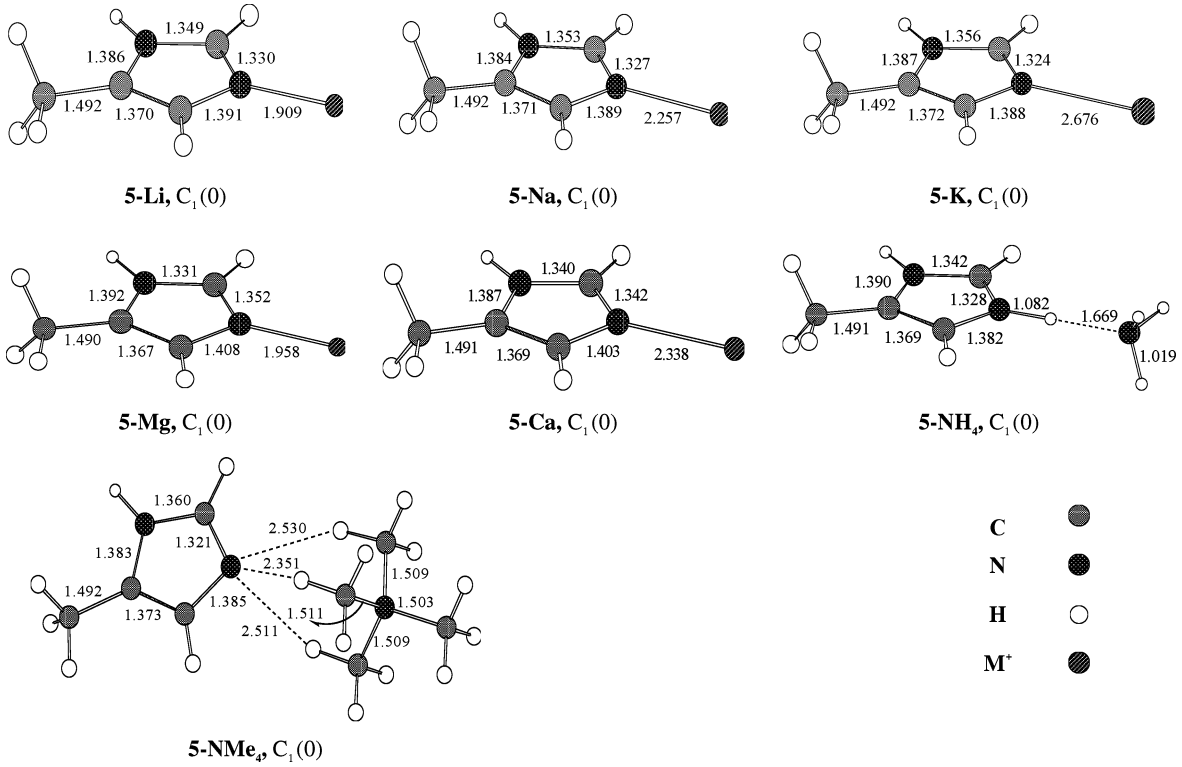

Figure 7. Optimized geometries (in Å) of **5-M** complexes at B3LYP/6-31G** level. The number of imaginary frequencies are given in parentheses.

TABLE 4: Mulliken Charges (in atomic units) of the Cations in the Cation−π Complexes Calculated at B3LYP/6-31G Level of Theory**

complex	Li	Na	K	Mg	Ca
1	0.428	0.651	0.844	0.938	1.493
2	0.417	0.643	0.841	0.912	1.478
3a	0.416	0.638	0.846	0.891	1.474
3b	0.684	0.773	0.881	1.208	1.606
4a	0.410	0.635	0.839	0.873	1.453
4b	0.512	0.701	0.865	1.002	1.517
5	0.753	0.813	0.886	1.505	1.700

(**1**−**5**) of the naturally occurring amino acids. The comparison of obtained interaction energies at various levels of theory to the existing experimental and theoretical results on the model system benzene indicate that B3LYP and MP2 methods with a split-valance triple-ζ basis set augmented with a set of polarization and diffuse functions for both heavy atoms and hydrogens yield qualitative accurate results to model the cation−π interactions. While proton prefers to bind selectively to one of the ring carbons of benzene ring, all the other metal cations as well as ammonium ions are found to form only π-complexes. The interaction energy decrease in the following order: **1-M** < **2-M** < **3-M** < **4-M** < **5-M**. Metal-wise the interaction energy variations are $Mg^{2+} > Ca^{2+} > Li^{+} > Na^{+} > K^{+} \cong NH_4^{+} > NMe_4^{+}$. While NH_4^{+} and NMe_4^{+} are capable of forming stable π-complexes, in the presence of electronegative heteroatoms the complexation is mostly through a strong hydrogen bonding interaction, resulting in the deviation of the trend. The interaction energy can be gauged by the structural changes upon complexation and the extend of charge transfer. In case of methyl imidazole, the nitrogen atom with lone pair in the molecular plane shows overwhelming affinity for all the cations, while for proton, the covalent complexation with the ring C situated between the two nitrogens has the highest affinity. While MP2 and DFT methods may give qualitatively correct trends in most cases, one need to go for more sophisticated levels of theory with adequate quality basis sets to get reliable results.[29] The present study reveal that cation−π interactions are extremely important and can be substantially stronger; however, when there is an alternative basic group, the covalent interaction appears to overtake the cation−π interaction. Importantly, the proton and metal ion complexation with the biological systems with aromatic motifs can be substantially different.

Acknowledgment. A.S.R. thanks CSIR for a senior research fellowship.

Supporting Information Available: Table S1 containing all the optimized coordinates at B3LYP/6-31G** level for all the structures considered in this study; Table S2 containing the components of the interaction energies at HF/6-31G* level calculated using Morokuma decomposition analysis. This material is available free of charge via the Internet at http://pubs.acs.org.

References and Notes

(1) Meyar, E. A.; Castellano, R. K.; Diederich, F. *Angew. Chem., Int. Ed.* **2003**, *42*, 1210.

(2) (a) Zakian, V. A. *Science* **1995**, *270*, 1601. (b) Rooman, M.; Lievin, J.; Bulsine, E.; Wintjens, R. *J. Mol. Biol.* **2002**, *319*, 67.

(3) (a) Dougherty, D. A.; Stauffer, D. A. *Science* **1990**, *250*, 1558. (b) Kumpf, R. A.; Dougherty, D. A. *Science* **1998**, *261*, 1708. (c) Ma, J. C.; Dougherty, D. A. *Chem. Rev.* **1997**, *97*, 1303.

(4) (a) Biot, C.; Wintjens, R.; Rooman, M. *J. Am. Chem. Soc.* **2004**, *126*, 6220. (b) McFail-Isom, L.; Shui, X.; Williams, L. D *Biochemistry* **1998**, *37*, 17105. (c) DeVos, A. M.; Ultsch, M.; Kosssiakoff, A. A. *Science* **1992**, *255*, 306.

(5) Cox, J. D.; Hunt, J. A.; Compher, K. M.; Fierke, C. A.; Christianson, D. W. *Biochemistry* **2000**, *39*, 13687.

(6) Stauffer, D. A.; Karlin, A. *Biochemistry* **1994**, *33*, 6840.

(7) (a) Meadows, E. S.; De Wall, S. L.; Barbour, L. J.; Gokel, G. W. *J. Am. Chem. Soc.* **2001**, *123*, 3092. (b) Macias, A. T.; Norton, J. E.; Evanseck, J. D. *J. Am. Chem. Soc.* **2003**, *125*, 2351.

(8) Kumar, M. K.; Rao, J. S.; Prabhakar, S.; Vairamani, M.; Sastry G. N. *Chem. Commun.* **2005**, 1420.

(9) (a) Hong, B. H.; Bae, S. C.; Lee, C.-W.; Jeong. S.; Kim, K. S. *Science* **2001**, *294*, 348. (b) Kim, K. S.; Tarakeshwar, P.; Lee, J. Y. *Chem.*

Rev. **2000**, *100*, 4145. (c) Choi, H. S.; Suh, S. B.; Cho, S. J.; Kim, K. S. *Proc. Natl. Acad. Sci. U.S.A.* **1998**, *95*, 12094. (d) Kim, D.; Tarakeshwar, P.; Kim, K. S. *J. Phys. Chem. A* **2004**, *108*, 1250. (e) Kim, D.; Hu, S.; Tarakeshwar, P.; Kim, K. S. *J. Phys. Chem. A* **2003**, *107*, 1228. (f) Hong, B. H.; Lee, J. Y.; Lee, C.-W.; Kim, J. C.; Bae, S. C.; Kim, K. S. *J. Am. Chem. Soc.* **2001**, *123*, 10748. (g) Kim, K. S.; Lee, J. Y.; Ha, T.-K.; Kim, D. H. *J. Am. Chem. Soc.* **1994**, *116*, 7399.

(10) (a) Gu, J.; Leszczynski, J. *J. Phys. Chem. A* **2001**, *105*, 10366. (b) Gu, J.; Leszczynski, J. *J. Phys. Chem. A* **2000**, *104*, 6308.

(11) (a) Tan, X. J.; Zhu, W. L.; Cui, M.; Luo, X. M.; Gu, J. D.; Silman, I.; Sussman, J. L.; Jiang, H. L.; Ji, R. Y.; Chen, K. X. *Chem. Phys. Lett.* **2001**, *349*, 113. (b) Cheng, Y. H.; Liu, L.; Fu. Y.; Chen, R.; Li, X. S.; Guo, Q. X. *J. Phys. Chem. A* **2002**, *106*, 11215.

(12) Woodin, R. L.; Beauchamp, J. L. *J. Am. Chem. Soc*. **1978**, *100*, 501.

(13) Guo, B. C.; Purnell, J. W.; Castleman, A. W., Jr. *Chem. Phys. Lett.* **1990**, *168*, 155.

(14) Sunner, J.; Nishizawa, K.; Kebarle, P. *J. Phys. Chem.* **1981**, *85*, 1814.

(15) Amicangelo, J. C.; Armentrout, P. B. *J. Phys. Chem. A* **2000**, *104*, 11420.

(16) (a) Feller, D. *Chem. Phys. Lett.* **2000**, *322*, 543. (b) Feller, D.; Dixon, D. A.; Nicholas, J. B. *J. Phys. Chem. A* **2000**, *104*, 11414. (c) Nicholas, J. B.; Hay, B. P.; Dixon, D. A. *J. Phys. Chem. A* **1999**, *103*, 1394.

(17) (a) Mo, Y.; Subramanian, G.; Gao, J.; Ferguson, D. M. *J. Am. Chem. Soc.* **2002**, *124*, 4832. (b) Rulisek, L.; Havlas, Z. *J. Am. Chem. Soc*. **2000**, *122*, 10428.

(18) Ryzhov, V.; Dunbar, R. C. *J. Am. Soc. Mass Spectrom.* **2000**, *11*, 1037.

(19) (a) Ruan, C.; Rodgers, M. T. *J. Am. Chem. Soc.* **2004**, *126*, 14600. (b) Amunugama, R.; Rodgers, M. T. *Int. J. Mass. Spectrom.* **2003**, *222*, 431. (c) Amunugama, R.; Rodgers, M. T. *J. Phys. Chem. A* **2002**, *106*, 5529.

(20) (a) Zhu, W.; Luo, X.; Puah, C. M.; Tan, X.; Shen, J.; Gu, J.; Chen, K.; Jiang, H. *J. Phys. Chem. A* **2004**, *108*, 4008. (b) Zhu, W.; Tan, X.; Shen, J.; Luo, X.; Cheng, F.; Mok, P. C.; Ji, R.; Chen, K.; Jiang, H. *J. Phys. Chem. A* **2003**, *107*, 2296. (c) Zhu, W.; Liu, T.; Shen, J.; Luo, X.; Tan, X.; Puah, C. M.; Jiang, H.; Chen, K. *Chem. Phys. Lett.* **2002**, *366*, 267.

(21) (a) Munoz, J.; Sponer, J.; Hobza, P.; Orozco, M.; Luque, F. J. *J. Phys. Chem. B* **2001**, *105*, 6051. (b) Sponer, J.; Burda, J. V.; Sabat, M.; Leszczynski, J.; Hobza, P. *J. Phys. Chem. A* **1998**, *102*, 5951. (c) Burda, J. V.; Sponer, J.; Leszczynski, J.; Hobza, P. *J. Phys. Chem. B* **1997**, *101*, 9670.

(22) (a) Garau, C.; Frontera, A.; Quinonero, D.; Ballester, P.; Costa, A.; Deya, P. M. *Chem. Phys. Lett.* **2004**, *392*, 85. (b) Garau, C.; Quinonero, D.; Frontera, A.; Costa, A.; Ballester, P.; Deya, P. M. *Chem. Phys. Lett.* **2003**, *370*, 7. (c) Quinonero, D.; Garau, C.; Frontera, A.; Ballester, P.; Costa, A.; Deya, P. M. *Chem. Phys. Lett.* **2002**, *359*, 486.

(23) (a) Tsuzuki, S.; Uchimaru, T.; Mikami, M. *J. Phys. Chem. A* **2003**, *107*, 10414. (b) Tsuzuki, S.; Uchimaru, T.; Mikami, M.; Tanabe, K. *J. Phys. Chem. A* **2002**, *106*, 3867. (c) Tsuzuki, S.; Honda, K.; Uchimaru, T.; Mikami, M.; Tanabe, K. *J. Am. Chem. Soc.* **2000**, *122*, 3746.

(24) (a) Ikuta, S. *J. Mol. Struct. (THEOCHEM)* **2000**, *530*, 201. (b) Hashimoto, S.; Ikuta, S. *J. Mol. Struct. (THEOCHEM)* **1999**, *468*, 85.

(25) (a) Priyakumar, U. D.; Sastry, G. N. *Tetrahedron Lett*. **2003**, *44*, 6043. (b) Priyakumar, U. D.; Punnagai, M.; Krishnamohan, G. P.; Sastry G. N. *Tetrahedron* **2004**, *60*, 3037.

(26) Boys, S. F.; Bernardi, R. *Mol. Phys.* **1979**, *19*, 553.

(27) Frisch, M. J.; Trucks, G. W.; Schlegel, H. B.; Scuseria, G. E.; Robb, M. A.; Cheeseman, J. R.; Montgomery, J. A., Jr.; Vreven, T.; Kudin, K. N.; Burant, J. C.; Millam, J. M.; Iyengar, S. S.; Tomasi, J.; Barone, V.; Mennucci, B.; Cossi, M.; Scalmani, G.; Rega, N.; Petersson, G. A.; Nakatsuji, H.; Hada, M.; Ehara, M.; Toyota, K.; Fukuda, R.; Hasegawa, J.; Ishida, M.; Nakajima, T.; Honda, Y.; Kitao, O.; Nakai, H.; Klene, M.; Li, X.; Knox, J. E.; Hratchian, H. P.; Cross, J. B.; Bakken, V.; Adamo, C.; Jaramillo, J.; Gomperts, R.; Stratmann, R. E.; Yazyev, O.; Austin, A. J.; Cammi, R.; Pomelli, C.; Ochterski, J. W.; Ayala, P. Y.; Morokuma, K.; Voth, G. A.; Salvador, P.; Dannenberg, J. J.; Zakrzewski, V. G.; Dapprich, S.; Daniels, A. D.; Strain, M. C.; Farkas, O.; Malick, D. K.; Rabuck, A. D.; Raghavachari, K.; Foresman, J. B.; Ortiz, J. V.; Cui, Q.; Baboul, A. G.; Clifford, S.; Cioslowski, J.; Stefanov, B. B.; Liu, G.; Liashenko, A.; Piskorz, P.; Komaromi, I.; Martin, R. L.; Fox, D. J.; Keith, T.; Al-Laham, M. A.; Peng, C. Y.; Nanayakkara, A.; Challacombe, M.; Gill, P. M. W.; Johnson, B.; Chen, W.; Wong, M. W.; Gonzalez, C.; Pople, J. A. *Gaussian 03*, revision A.1; Gaussian, Inc.: Wallingford, CT, 2004.

(28) (a) Fujii, A.; Morita, S.; Miyazaki, M.; Ebata, T.; Mikami, N. *J. Phys. Chem. A* **2004**, *108*, 2652. (b) Cheng, J.; Kang, C.; Zhu, W.; Luo, X.; Puah, C. M.; Chen, K.; Shen, J.; Jiang, H. *J. Org. Chem.* **2002**, 6*8*, 7490. (c) Zhu, W.; Jiang, H.; Puah, C. M.; Tan, X.; Chen, K.; Cao, Y.; Ji. R. *Perkins Trans. 2* **1999**, 2615.

(29) (a) Muller-Dethlefs, K.; Hobza, P. *Chem. Rev.* **2000**, *100*, 143. (b) Rappe, A. K.; Bernstein, E. R. *J. Phys. Chem. A* **2000**, *104*, 6117.